



## Evaluating the performance of a simple phenomenological model for online forecasting of ammonium concentrations at WWTP inlets

**Vezzaro, Luca; Pedersen, Jonas Wied; Larsen, Laura Holm; Thirsing, Carsten; Duus, Lene Bassø; Mikkelsen, Peter Steen**

*Published in:*  
Water Science and Technology

*Link to article, DOI:*  
[10.2166/wst.2020.085](https://doi.org/10.2166/wst.2020.085)

*Publication date:*  
2020

*Document Version*  
Peer reviewed version

[Link back to DTU Orbit](#)

*Citation (APA):*  
Vezzaro, L., Pedersen, J. W., Larsen, L. H., Thirsing, C., Duus, L. B., & Mikkelsen, P. S. (2020). Evaluating the performance of a simple phenomenological model for online forecasting of ammonium concentrations at WWTP inlets. *Water Science and Technology*, 81(1), 109–120. <https://doi.org/10.2166/wst.2020.085>

---

### General rights

Copyright and moral rights for the publications made accessible in the public portal are retained by the authors and/or other copyright owners and it is a condition of accessing publications that users recognise and abide by the legal requirements associated with these rights.

- Users may download and print one copy of any publication from the public portal for the purpose of private study or research.
- You may not further distribute the material or use it for any profit-making activity or commercial gain
- You may freely distribute the URL identifying the publication in the public portal

If you believe that this document breaches copyright please contact us providing details, and we will remove access to the work immediately and investigate your claim.

---

1  
2 **Evaluating the performance of a simple phenomenological**  
3 **model for online forecasting of ammonium concentrations at**  
4 **WWTP inlets**  
5  
6

7 Luca Vezzaro<sup>1,2</sup>, Jonas Wied Pedersen<sup>2</sup>, Laura Holm Larsen<sup>2</sup>, Carsten Thirring<sup>3</sup>, Lene Bassø Duus<sup>4</sup>, and  
8 Peter Steen Mikkelsen<sup>2</sup>  
9

10  
11 <sup>1</sup>Krüger A/S, Veolia Water Technologies, Gladsaxevej 363, 2860 Søborg, Denmark (Email: *lxv@kruger.dk*)

12 <sup>2</sup>Department of Environmental Engineering (DTU Environment), Technical University of Denmark, Building 115,  
13 2800 Kongens Lyngby, Denmark (Email: *jowi@env.dtu.dk;psmi@env.dtu.dk*)

14 <sup>3</sup>BIOFOS A/S, Refshalevej 250, 1432 København K, Denmark (Email: *ct@biofos.dk*)

15 <sup>4</sup>Aarhus Vand A/S, Gunnar Clausens Vej 34, 8260 Viby J, Denmark (Email: *lba@aarhusvand.dk*)  
16

17 **Abstract**

18 A simple model for online forecasting of ammonium (NH<sub>4</sub><sup>+</sup>) concentrations in sewer systems is  
19 proposed. The forecast model utilizes a simple representation of daily NH<sub>4</sub><sup>+</sup> profiles and the  
20 dilution approach combined with information from online NH<sub>4</sub><sup>+</sup> and flow sensors. The method  
21 utilizes an ensemble approach based on past observations to create model prediction bounds. The  
22 forecast model was tested against observations collected at the inlet of two WWTPs over an 11-  
23 month period. NH<sub>4</sub><sup>+</sup> data were collected with ion-selective sensors. The model performance  
24 evaluation focused on applications in relation to online control strategies. The results of the  
25 monitoring campaigns highlighted a high variability in daily NH<sub>4</sub><sup>+</sup> profiles, stressing the  
26 importance of an uncertainty-based modelling approach. The maintenance of the NH<sub>4</sub><sup>+</sup> sensors  
27 resulted in important variations of the sensor signal, affecting the evaluation of model structure  
28 and its performance. The forecast model succeeded in providing outputs that potentially can be  
29 used for integrated control of wastewater systems. This study provides insights on full scale  
30 application of online water quality forecasting models in sewer systems. It also highlights several  
31 research gaps which - if further investigated - can lead to better forecasts and more effective real-  
32 time operations of sewer and WWTP systems.  
33

34 **Keywords**

35 Automatic parameter estimation, Sensor maintenance, Ensemble-based model predictions, Water  
36 Quality-based control  
37  
38

39 **INTRODUCTION**

40 Models for forecasting water quality in different parts of the integrated urban drainage-wastewater  
41 system (sewers, wastewater treatment plants - WWTP) can provide useful information for  
42 improving the operation of integrated urban drainage-wastewater systems (Yuan et al., 2019). These  
43 models can be used to quantify discharges from Combined Sewer Overflows (CSO), or in an online  
44 context as part of real-time control strategies aiming at optimizing WWTP operations (the so-called  
45 “software sensors” – e.g. Stentoft et al. (2017)). Further potential applications include Model  
46 Predictive Control approaches, allowing water quality based control of sewer systems (e.g. Vezzaro  
47 et al., 2013) or WWTPs (Stentoft et al., 2019) over different forecast horizons.  
48

49 As pointed out in Langeveld et al. (2017), the increased availability of long-term times series of  
50 water quality parameters with high resolution in time (e.g. Schilperoort et al., 2012; Métadier and  
51 Bertrand-Krajewski, 2012; Alferes et al., 2013) allows the development of new models utilizing  
52 such information. There is a wide experience with the application of data-driven software sensors in  
53 WWTPs (Haimi et al., 2013; Newhart et al., 2019), and several studies on simulating WWTP  
54 influent quality (Martin and Vanrolleghem, 2014). Many of these studies employ  
55 empirical/phenomenological approaches (Langeveld et al., 2017; Gernaey et al., 2011;

---

56 Langergraber et al., 2008), while Talebizadeh et al. (2016) proposed a stochastic influent generator  
57 to provide a more realistic description of the natural variability of WWTP influent. These examples  
58 are mostly based on offline simulation studies, using pre-validated data (e.g. Flores-Alsina et al.,  
59 2014), a condition that is not available under actual real-time conditions. The majority of research  
60 on forecasting of water quality indicators at WWTPs focuses on quantities within the process tanks  
61 or at the plant outlet. Few examples deal with predictions of the WWTP influent (e.g. Kusiak et al.,  
62 2013; Yu et al., 2018), despite its potential use in feed-forward control. Furthermore, model  
63 predictive power is often evaluated in terms of statistical assumptions regarding residuals, while  
64 online application requires more robust, *ad-hoc* metrics, focusing on the intended use of the model  
65 outputs.

66  
67 This paper presents a simple phenomenological model specifically developed for online prediction  
68 of ammonium ( $\text{NH}_4^+$ ) loads and concentrations along with their uncertainty. The model relies on a  
69 flow forecast and continuous online  $\text{NH}_4^+$  measurements from an ISE (ion-selective electrode)  
70 sensor. In the evaluation of forecast skill in this study, the forecasts of ammonia loads are based on  
71 *ex-post flow forecasts*, i.e. measured flow values that are used “as if” they are forecasted values. In  
72 an operational setup, the measured flow should obviously be exchanged for real-time forecasts of  
73 flow. However, the *ex-post* setup in this paper ensures that the performance evaluation of the  
74 ammonium forecasts is independent of errors in the flow domain. The forecasts are tested at the  
75 inlet of two Danish WWTPs and the performance of the forecast model is evaluated over an 11-  
76 month period. The evaluation also aims at identifying further research gaps and improvements with  
77 specific focus on application in online control strategies.

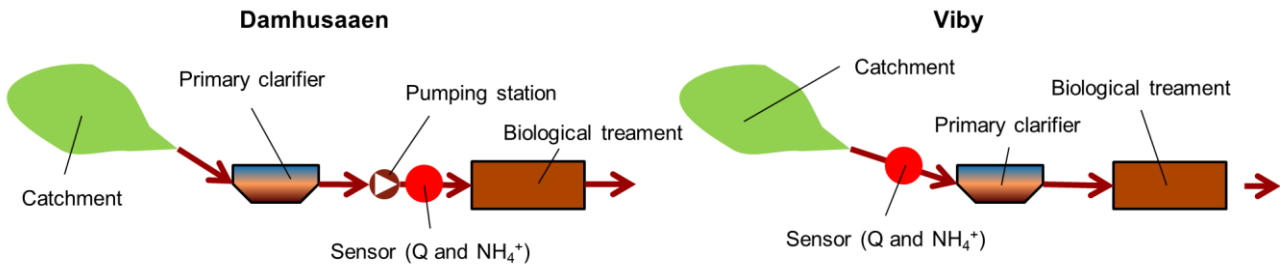
## 78 79 80 **MATERIAL AND METHODS**

### 81 82 **Water quality monitoring**

83 Flow and ammonia measurements have been collected with a 2-minute frequency at the Viby  
84 WWTP (Aarhus, Denmark – since June 2018) and the Damhusaaen WWTP (Copenhagen, Denmark  
85 – since April 2018). The Viby catchment consists of 6.78 km<sup>2</sup> combined and 7.48 km<sup>2</sup> separate  
86 systems (Ahm et al., 2013). The majority of the system is gravity driven, while the flow from two  
87 minor subcatchments is pumped to the plant. The Damhusaaen WWTP receives wastewater from a  
88 67 km<sup>2</sup> combined system, which is mainly gravity driven (flow from an adjacent catchment can be  
89 pumped in case of extreme events).

90  
91  $\text{NH}_4^+$  is measured with commercially available ion-selective sensors (Table S1). The sensors in  
92 Viby and in Damhusaaen are placed at different locations of the plants for logistical reasons (Figure  
93 1): after the primary clarifier and a pumping station in Damhusaaen and after the grit removal in  
94 Viby (Table 1). Their planned sensor maintenance follows different schedules (Table 1). Data from  
95 the plants’ SCADA systems are transferred to the AQUAVISTA<sup>TM</sup> cloud-based system (based on  
96 the STAR<sup>®</sup> system described in Nielsen and Onnerth, 1995), where they are automatically quality  
97 controlled based on simple rule methods (e.g. running variance, physical ranges, flat lines).

98



99  
100 **Figure 1.** Schematic placement of the sensors in the two plant layouts.  
101

102 **Table 1.** Relevant information for the two WWTPs included in the study.

	Damhusaaen	Viby WWTP
Sensor placement (Figure 1)	After primary clarifier and pumping station	At plant inlet (after grit removal)
Planned sensor cleaning and performance check	Weekly	Weekly
Sensor calibration	If sensor deviation from lab measurements >10%	If sensor deviation from lab measurements >5%
Start of monitoring campaign	April 2018	June 2018
Threshold used to define wet weather events (at WWTP inlet)	5000 m <sup>3</sup> /hr	400 m <sup>3</sup> /hr
Forecast model parameters		
Fourier series coefficients	X	X
Volume of primary clarifier	X	
Additional morning pulse		X

103  
104 **Forecast model**

105 *Ammonium Forecasts.* The proposed forecast model is schematized in Figure 2 and further  
106 explained in the following paragraphs. The proposed model builds upon the widely applied concept  
107 of daily ammonium loads (Figure 2a), i.e. the concept that NH<sub>4</sub><sup>+</sup> loads (i) only originate from  
108 domestic sources that can vary between weekdays and weekends, (ii) follow a typical diurnal  
109 profile over 24 hours, and (iii) are unaffected by wet weather events (e.g. Langeveld et al., 2017;  
110 Martin and Vanrolleghem, 2014; Langergraber et al., 2008). The NH<sub>4</sub><sup>+</sup> loads are estimated on a  
111 daily basis for dry days (Figure 2b), and forecast are generated by using an ensemble approach,  
112 utilizing the daily load profiles from *n* previous dry days (Figure 2c). By combining the NH<sub>4</sub><sup>+</sup> loads  
113 with flow data it is then possible to estimate NH<sub>4</sub><sup>+</sup> concentrations by using a simple dilution  
114 approach.  
115

116 The model uses a moving window of length *n* on previous dry days (Figure 2a). Here, dry days are  
117 defined with respect to the flow observations, and not simply as days without rain events. Wet days  
118 are defined as the days when the measured flow exceeded the flow threshold that is used to activate  
119 the wet weather controls at the plant (Table 1). Days with small rain events, generating flows below  
120 the threshold, would therefore be classified as dry days, since they would not lead to a change in the  
121 plant operations. In daily operation, the threshold value depends on the plant characteristics and  
122 status (based e.g. on actual capacity of the biological treatment and settling conditions in the  
123 secondary clarifier). Once the flow falls back below the threshold, the following 12 hours (24 hours  
124 if the event volume is above 20,000 m<sup>3</sup>) are still characterized as wet periods. This is done because  
125 NH<sub>4</sub><sup>+</sup> concentrations are still affected by slow catchment runoff and concentrations are still below  
126 typical dry weather values.  
127

128 The operational cycle for the online forecast model on the  $i$ -th day are described by the following  
129 steps (Figure 2b,c):

130 *Step 1:* A few minutes after midnight, flow measurements from day  $i-1$  are analysed for identifying  
131 potential wet weather events.

132 *Step 2:* If the previous day was a dry day, the parameters of the  $\text{NH}_4^+$  daily profile for day  $i-1$  are  
133 estimated and stored in a database (Figure 2b).

134 *Step 3:* Estimated parameter sets from the previous  $n$  dry days of corresponding day type  
135 (weekday/weekend) are retrieved from the database.

136 *Step 4:* Ammonium forecasts for day  $i$  are generated by running the model every two minutes.  
137 Forecast uncertainty is created as an ensemble with  $n$  members consisting of ammonia load profiles  
138 from the past  $n$  corresponding days (weekday/weekend) (Figure 2c).

139 As shown in Figure 2c, these steps are repeated for each day by shifting the moving window and by  
140 repeating Steps 1-4.

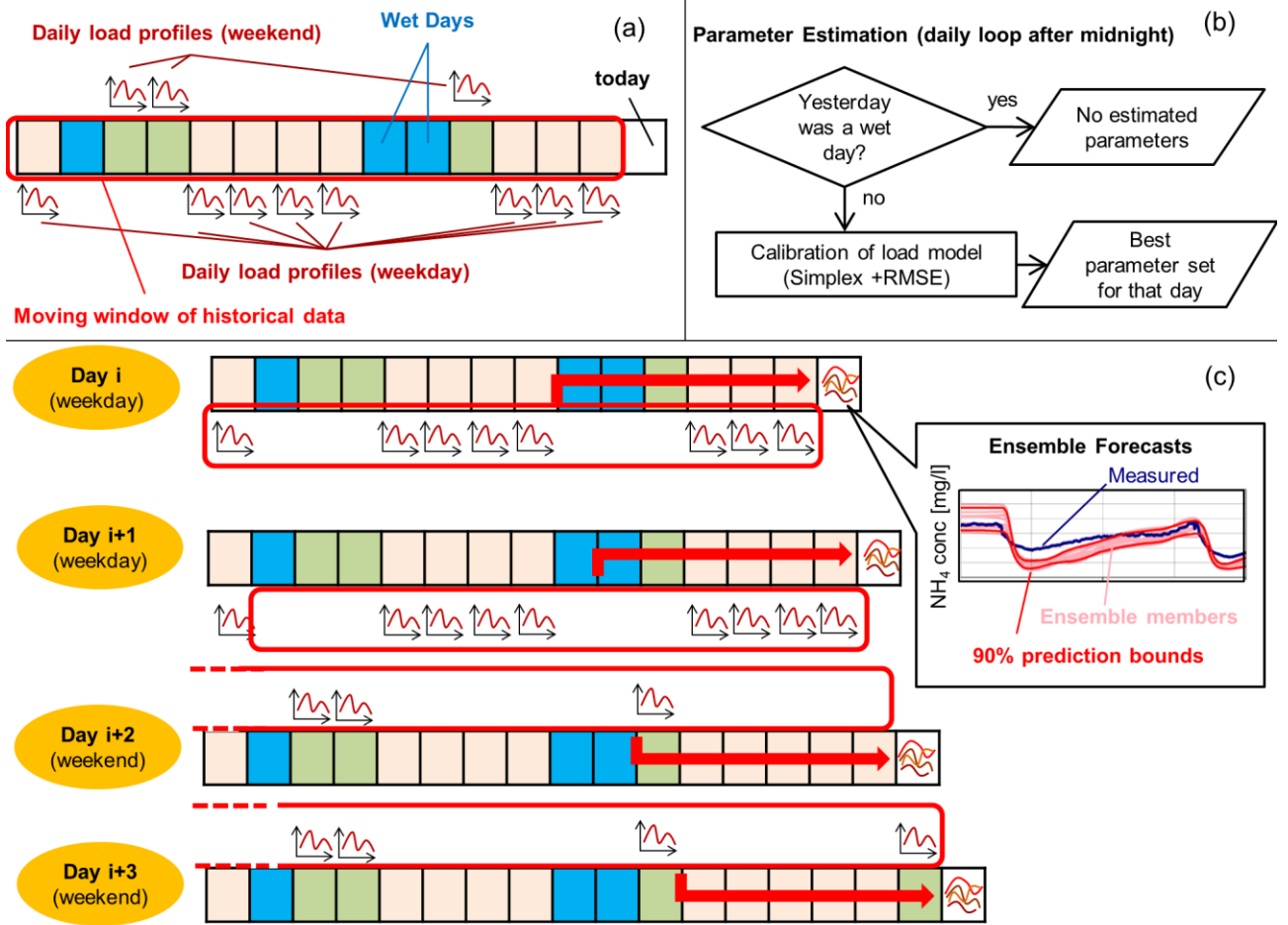
141  
142 *Model structure.* The online model runs in two-minute time steps and uses a Fourier series to  
143 represent the diurnal variation of the  $\text{NH}_4^+$  load ( $F_{\text{NH}_4}(t)$  [ $\text{g}_{\text{NH}_4}/\text{hr}$ ]) over a day (as in Bechmann et  
144 al., 1999):

$$145 \quad F_{\text{NH}_4}(t) = \alpha_0 + \sum_{k=1}^2 (\alpha_k \sin(2\pi kt) + \beta_k \cos(2\pi kt)) \quad (1)$$

147  
148 where  $\alpha_0, \alpha_1, \alpha_2$  and  $\beta_1, \beta_2$  are the Fourier coefficients [ $\text{g}_{\text{NH}_4}/\text{hr}$ ], and the time  $t$  is expressed as fraction  
149 of a day [-]. This formulation of the Fourier series is widely applied in WWTP influent modelling  
150 since it provides the typical pattern observed in domestic wastewater (e.g. Langergraber et al.  
151 (2008)), with a peak in the morning and a second smaller peak in the late afternoon/evening.  
152 Ammonium concentrations  $S_{\text{NH}_4}$  [ $\text{g}_{\text{NH}_4}/\text{m}^3$ ] are then calculated by dividing the estimated loads by  
153 the flow  $Q(t)$  [ $\text{m}^3/\text{hr}$ ], as in Langeveld et al. (2017):

$$154 \quad S_{\text{NH}_4}(t) = F_{\text{NH}_4}(t)/Q(t) \quad (2)$$

155  
156  
157 As mentioned earlier, the flow values  $Q(t)$  that are used as input to the forecasting scheme are the  
158 values that were observed later in the day, and thus not real forecasts of the flow (also referred to as  
159 *ex-post* forecasts).



160  
 161 **Figure 2.** Conceptual schematization of the proposed forecast setup: (a) moving window of  
 162 historical data (in this example with  $n = 8$  days) and classification into weekdays, weekends, and  
 163 wet days; (b) procedure for parameter estimation (run every day after midnight); (c) example  
 164 showing how the forecast model is applied for a period from day  $i$  to day  $i+3$ .  
 165

166 Given the specific setup at the Damhusaaen site, the volume of the primary clarifiers (about 12,000  
 167  $m^3$ ) is included in the model as it leads to a time delay and to an attenuation of ammonium profiles  
 168 between the inlet and the sensor location. To account for these issues, the estimated  $NH_4^+$  loads at  
 169 the inlet (from eq. 1) are routed through three cascading Continuously Stirred Tank Reactors.

170  
 171 The  $NH_4^+$  concentration is then calculated by looking at the outlet of the last tank (eq. 3d). The mass  
 172 balance of the three tanks is:  
 173

174 
$$\frac{dM_{1,SNH_4}}{dt} = F_{NH_4} - \frac{M_{1,SNH_4}}{V} Q \quad (3a)$$

175 
$$\frac{dM_{2,SNH_4}}{dt} = (M_{1,SNH_4} - M_{2,SNH_4}) \frac{Q}{V} \quad (3b)$$

176 
$$\frac{dM_{3,SNH_4}}{dt} = (M_{2,SNH_4} - M_{3,SNH_4}) \frac{Q}{V} \quad (3c)$$

177 
$$S_{NH_4}'(t) = M_{3,SNH_4}(t)/V \quad (3d)$$

178  
 179 where  $V [m^3]$  is the volume of each tank (kept as a calibration parameter), and  $M_i [kg]$  are the mass  
 180 of  $NH_4^+$  as model states.  
 181

182 Furthermore, a preliminary analysis of the  $\text{NH}_4^+$  loads measured at the Viby WWTP showed how  
 183 the morning peak was characterized by a quite steep increase between 08:00 and 10:00. Since the  
 184 Fourier series used by the model (eq. 1) encountered difficulties in representing such behaviour, an  
 185 additional ammonium “pulse” was added. This is represented by an asymmetrical term, built by  
 186 transforming of a Gaussian bell function (centred in the morning peak) into an asymmetrical pulse:  
 187

$$188 \quad F'_{\text{NH}_4}(t) = F_{\text{NH}_4}(t) + \gamma_1 e^{(-\gamma_2(\log_{10}(t) - \log_{10}(\gamma_3)))^2} \quad (4)$$

189 where  $\gamma_1$  [g/hr] provides the magnitude of the additional peak (equivalent to a mass added to mimic  
 190 the steep increase),  $\gamma_2$  [-] defines the duration of the peak, and  $\gamma_3$  [-] the timing of the extra peak,  
 191 constrained to be between 07:00 and 11:00 (still expressed as fraction of a day). Compared to a  
 192 tabular description of the daily profile (as in Langeveld et al., 2017), this formulation was chosen to  
 193 obtain a profile closer to the observations without significantly increasing the number of  
 194 parameters.  
 195

196  
 197 *Estimation of model parameters.* The model parameters are estimated by using an optimization  
 198 routine based on the Simplex method, minimizing the Root Mean Square Error (RMSE) between  
 199 simulated and observed loads. The optimization is run once per day (just after midnight), using the  
 200 data collected in the previous 24 hours. An optimal parameter set for the load model ( $\theta_{opt,i}$ ) is  
 201 obtained for each calendar day. It is assumed that rain-induced phenomena (e.g. first flush, WWTP  
 202 inlet bypass) would affect the estimation of the  $\text{NH}_4^+$  profiles. Therefore, the optimization  
 203 procedure is not run for wet days, i.e. for days when the plant would operate in wet-weather mode.  
 204 Days characterized by small rain events, generating flows below the threshold, are classified as dry  
 205 periods, and thereby included in the calibration.  
 206

## 207 **Evaluation of model performance**

208 *Experimental setup.* The proposed forecast model was tested on the data collected from June 2018  
 209 to May 2019 (i.e. the performance evaluation covered 318 days for both locations). Online  
 210 operations were mimicked by following the procedure described earlier (Figure 2c).  
 211

212 *Performance evaluation.* The model performance was calculated on a daily basis by comparing  
 213 measured  $\text{NH}_4^+$  concentrations against the output of the model for the specific  $i$ -th day. Two  
 214 performance indicators were used: the Mean Absolute Relative Error (MARE) for evaluating the  
 215 performance of the ensemble median forecast, and the coverage of observations to evaluate the skill  
 216 of the ensemble spread:  
 217

$$218 \quad MARE = \frac{1}{k} \sum_{i=1}^k \left| \frac{S_{\text{NH}_4, \text{sim}, i} - S_{\text{NH}_4, \text{obs}, i}}{S_{\text{NH}_4, \text{obs}, i}} \right| \quad (5)$$

$$219 \quad \text{Coverage} = \frac{1}{k} \sum_{i=1}^k I_i \quad \text{with} \quad \begin{cases} I_i = 0 \text{ for } S_{\text{NH}_4, \text{sim}05, i} > S_{\text{NH}_4, \text{obs}, i} \text{ or } S_{\text{NH}_4, \text{sim}95, i} < S_{\text{NH}_4, \text{obs}, i} \\ I_i = 1 \text{ for } S_{\text{NH}_4, \text{sim}05, i} < S_{\text{NH}_4, \text{obs}, i} < S_{\text{NH}_4, \text{sim}95, i} \end{cases} \quad (6)$$

220  
 221 Where  $k$  is the number of simulated values;  $S_{\text{NH}_4, \text{obs}, i}$  is the  $i$ -th observation;  $S_{\text{NH}_4, \text{sim}, i}$  is the  
 222 median of the simulated values at the  $i$ -th time step;  $S_{\text{NH}_4, \text{sim}05, i}$  and  $S_{\text{NH}_4, \text{sim}95, i}$  are the 5% and the  
 224 95% percentile of the simulated values for the same time step, respectively.  
 225

226 Among the potential applications of the online forecast model, the following options were  
 227 hypothesized in order to investigate the performance during wet-weather events:

- 
- 228 • Estimation of incoming ammonium loads, including potential first-flush peaks from the  
229 upstream catchment (as described by e.g. Krebs et al., 1999). Such forecasts can potentially be  
230 used to optimize the removal efficiency of the WWTP by using a Model Predictive Control (e.g.  
231 Stenoft et al., 2019).
- 232 • Estimation of ammonium dilution during a rain event. This information might open the  
233 possibility for water-quality based controls involving prioritizing bypass or diverting low  
234 pollution flows to natural waters, as described by e.g. Hoppe et al. (2011).
- 235

236 In the first case, the relative error was calculated on the ammonium load for the first 30 minutes of a  
237 rain event. In the second case, a contingency table (Bennett et al., 2013) was used to evaluate the  
238 ability of the forecast model to estimate dilution in the plant influent. Dilution is here defined a 10%  
239 drop of concentration below dry weather values (e.g. if dry weather concentration is 40 mg/l, a  
240 dilution event starts when the concentration drops below 36 mg/l). Since ammonium concentrations  
241 vary throughout the day and sensor measurements are affected by variability and outliers, the dry  
242 weather concentration threshold was defined as the 5<sup>th</sup> percentile concentration measured during the  
243 2 hours before the start of the event.

244

## 246 **RESULTS AND DISCUSSION**

### 248 **Measurement campaigns**

249 The available datasets from the two plants are shown in Figure 3a-d. A total of 35 and 57 wet  
250 weather events were observed in Damhusaaen and Viby, respectively. Based on the analysis of the  
251 rainfall data recorded in the catchments (see Supplementary Information – Table S2), wet-weather  
252 events were caused by rainfall greater than 3-4 mm (Damhusaaen) and 2 mm (Viby).

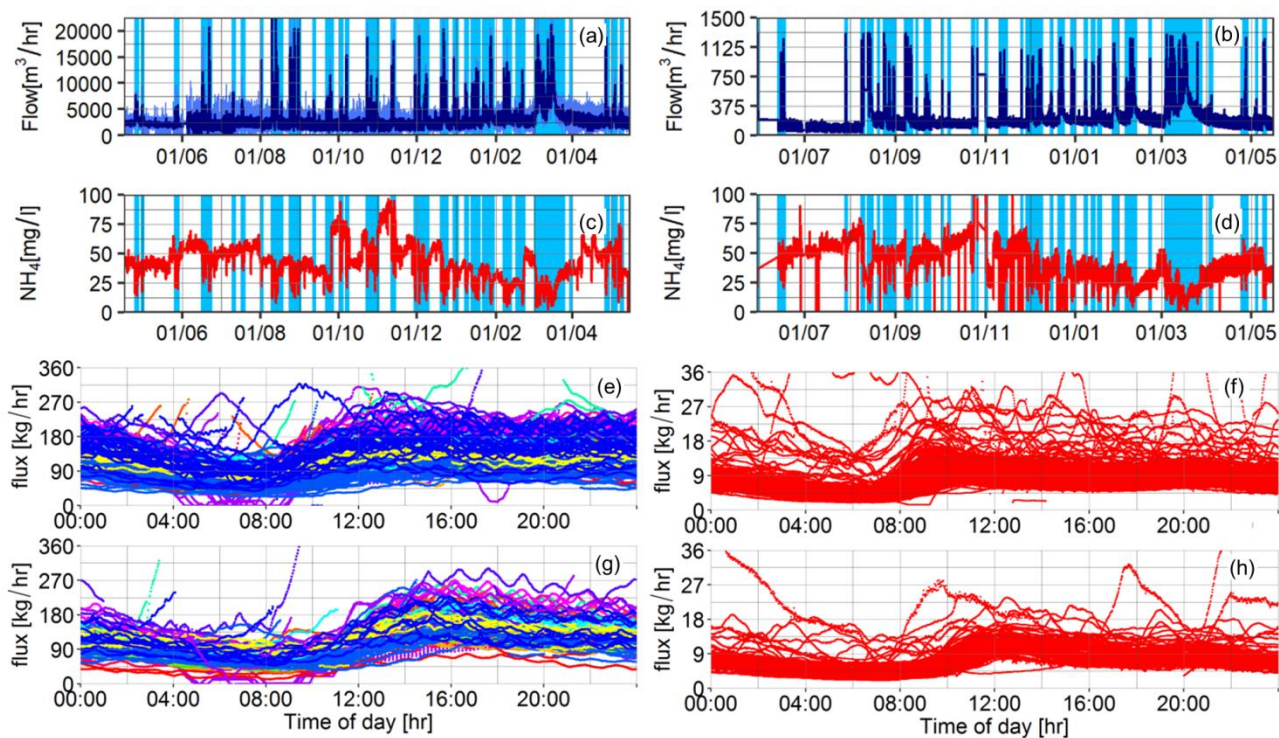
253

254 The data at the Damhusaaen WWTP show the influence of the sensor's location within the plant  
255 (Figure 1), as the flow (light blue in Figure 3a) is affected by a pumping station, showing spikes  
256 often exceeding the wet-weather threshold (see an example in Figure S1). To avoid data artefacts  
257 and false identification of wet-weather events, flow measurements were smoothed to estimate the  
258 WWTP inlet flow. Flow data were filtered by using a simple moving average with 60 steps (dark  
259 blue). The daily variations in  $\text{NH}_4^+$  concentrations are clearly attenuated by the volume of the  
260 primary clarifier, as daily variations ranged in the order of 5-10 mg/l, and a distinct diurnal pattern  
261 is not evident (Figure S1). Conversely, the data from the Viby WWTP show the characteristic daily  
262 patterns associated with dry-weather WWTP inlets, with an evident morning peak and daily  
263 variations of more than 15 mg/l (Figure S2).

264

265 Effects of sensor calibration in Damhusaaen is seen in the sudden changes in  $\text{NH}_4^+$  concentrations,  
266 which in the most extreme cases can jump more than 20 mg/l before and after the calibration. This  
267 is consistent with the observations in Ceconi et al. (2019), who highlighted the (potentially  
268 negative) influence of the sensor calibration on the sensor readings. The effect of the different  
269 calibrations can be seen in the calculated ammonium load profiles (Figure 3e,g), which shows  
270 variations in the average daily level. Nevertheless, the daily load profiles measured at both  
271 Damhusaaen (Figure 3e,g) and Viby (Figure 3f,h) show a great inter-day variability. An approach  
272 based on e.g. only tabular values or fixed ammonium profiles, neglecting the natural variability of  
273 the simulated process, would be affected by important uncertainty. This stresses the importance of  
274 the proposed ensemble approach to generate model prediction bounds and allow for a more  
275 confident application of model forecast for online applications.

276



277  
278  
279  
280  
281  
282  
283

**Figure 3.** Overview of the measured flow (a,b) and ammonium concentrations (c,d) at Damhusaen (left column) and Viby (right column). Light blue line: raw flow data; dark blue line: filtered flow data. Wet weather events are shown with light blue background. Measured ammonium loads for weekdays (e,f) and weekends (g,h). Fluxes measured during different calibration periods in Damhusaaen (e,g) are shown by using different colour codes.

284  
285  
286  
287  
288  
289  
290  
291  
292  
293  
294  
295

### Performance during the entire period

The performance of the forecast model over the whole analysed period is shown in Figure 4 where each red dot represents the average skill over a single day. Figure 4 shows how the sensor maintenance resulted in a deterioration of the forecast model performance after the signal correction. In fact, after calibration MARE tends to increase (Figure 4a), while the coverage drops (Figure 4b). This is explained by the fact the model uses a moving window of values preceding the forecast, which may include days where sensor calibration takes place. Predictions after a sensor recalibration event consistently over- or underestimating the  $\text{NH}_4^+$  concentrations compared to the signal after the sensor is calibrated. Subsequently, prediction improves in the days following the calibration, as the window moves further, including an increasing number of days with the new sensor calibration and thereby discarding values from the “old” calibration.

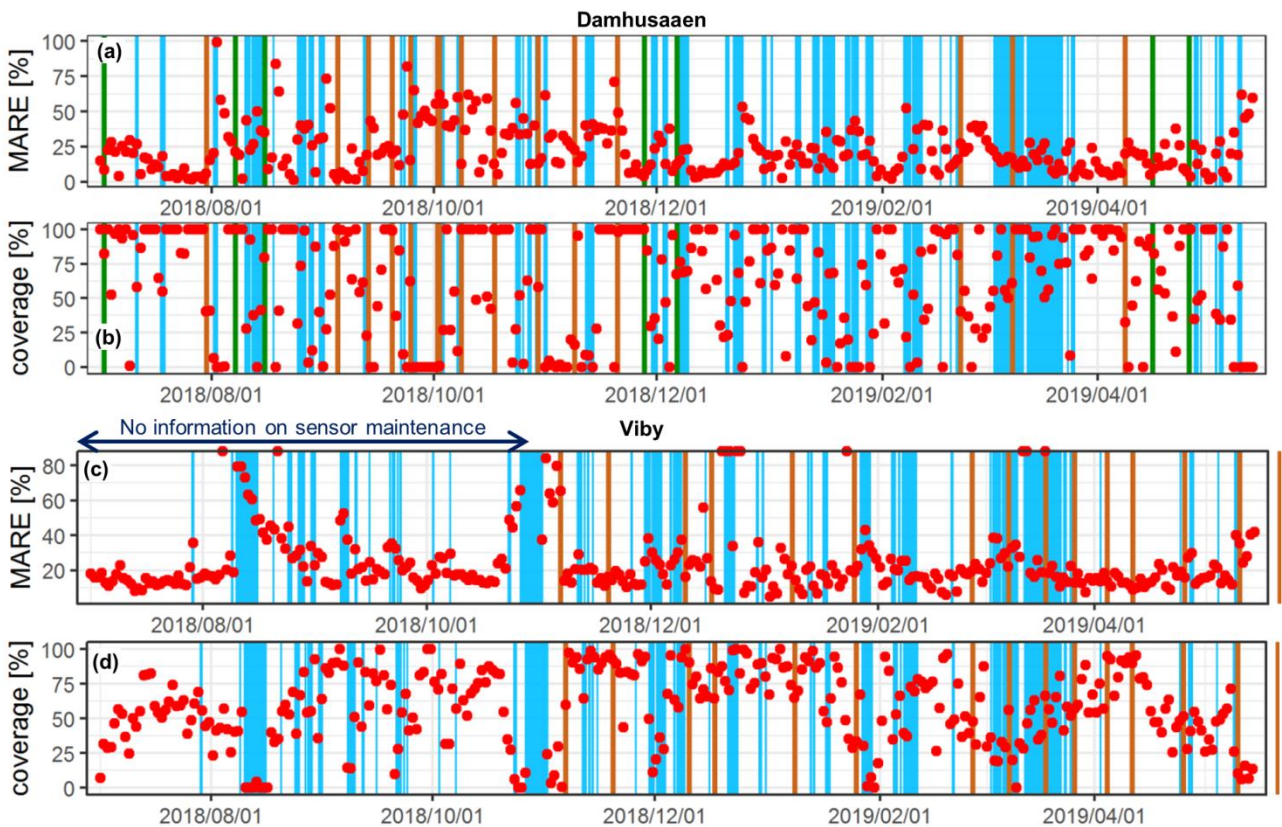
296  
297  
298  
299  
300  
301  
302  
303  
304  
305  
306  
307

It should be noted that in some periods, sensor maintenance was performed with a frequency lower than planned: e.g. no sensor maintenance was performed in Damhusaaen in the period from mid-December to mid-February. Although a small drift in the sensor reading can be theorized (Figure S3), no significant worsening of model performance was observed in this period. This can be explained by the chosen ensemble approach, which only considers data from the latest  $n$  dry days. Potential drift of the sensor is assimilated by the moving window, ensuring a good agreement between measured and modelled data. This highlights the importance of adopting a data validation routine capable of detecting sensor drift in an online setup and/or correcting sensor data. A similar behaviour can be observed in March, when an exceptionally long rainy period led to an important increase of groundwater infiltration and thereby to a drop in  $\text{NH}_4^+$ . Also in this case, the model performance did not show important variations compared to other periods. It can be assumed that using a greater value of  $n$  will result in a deterioration of model performance in case of sensor drift

308 or increase/decrease of the  $\text{NH}_4^+$  dilution due to groundwater infiltration. A smaller value of  $n$  might  
309 on the other hand make the ensemble predictions overly sensitive to inter-daily variations.

310  
311 Results from Viby (Figure 4c,d) show a deterioration of the forecast model performance following  
312 wet weather events. In the periods when the forecast model provided the best performance, MARE  
313 ranged at 20-25% for both the plants, while the coverage was better in Damhusaaen (often  
314 achieving 100%). This can be explained by the difficulties in the proposed model structure to fully  
315 describe the specific daily ammonium pattern in Viby. The performance of the forecast model in  
316 terms of coverage could be improved by either increasing the length of the moving window (i.e. by  
317 increasing the number of ensemble members and thereby the width of the model prediction bounds)  
318 or by modifying the model structure (i.e. identifying a better equation than eq. 4). However, the first  
319 option would not lead to an improvement in MARE. This is likely to be achieved by the latter  
320 option which, however, should find a trade-off between model complexity (i.e. the number of model  
321 parameters) and the computational requirements for a cloud-based system. For example, several  
322 commercial software products, often applied in an offline context, simulate wastewater generation  
323 by using tabular hourly values. This formulation would clearly ensure a better representation of the  
324 daily profile. However, running an automatic optimization routine for 24 parameters might be  
325 computationally demanding or have identifiability problems: therefore, such formulation is not  
326 preferable in an online, cloud-based setup.

327



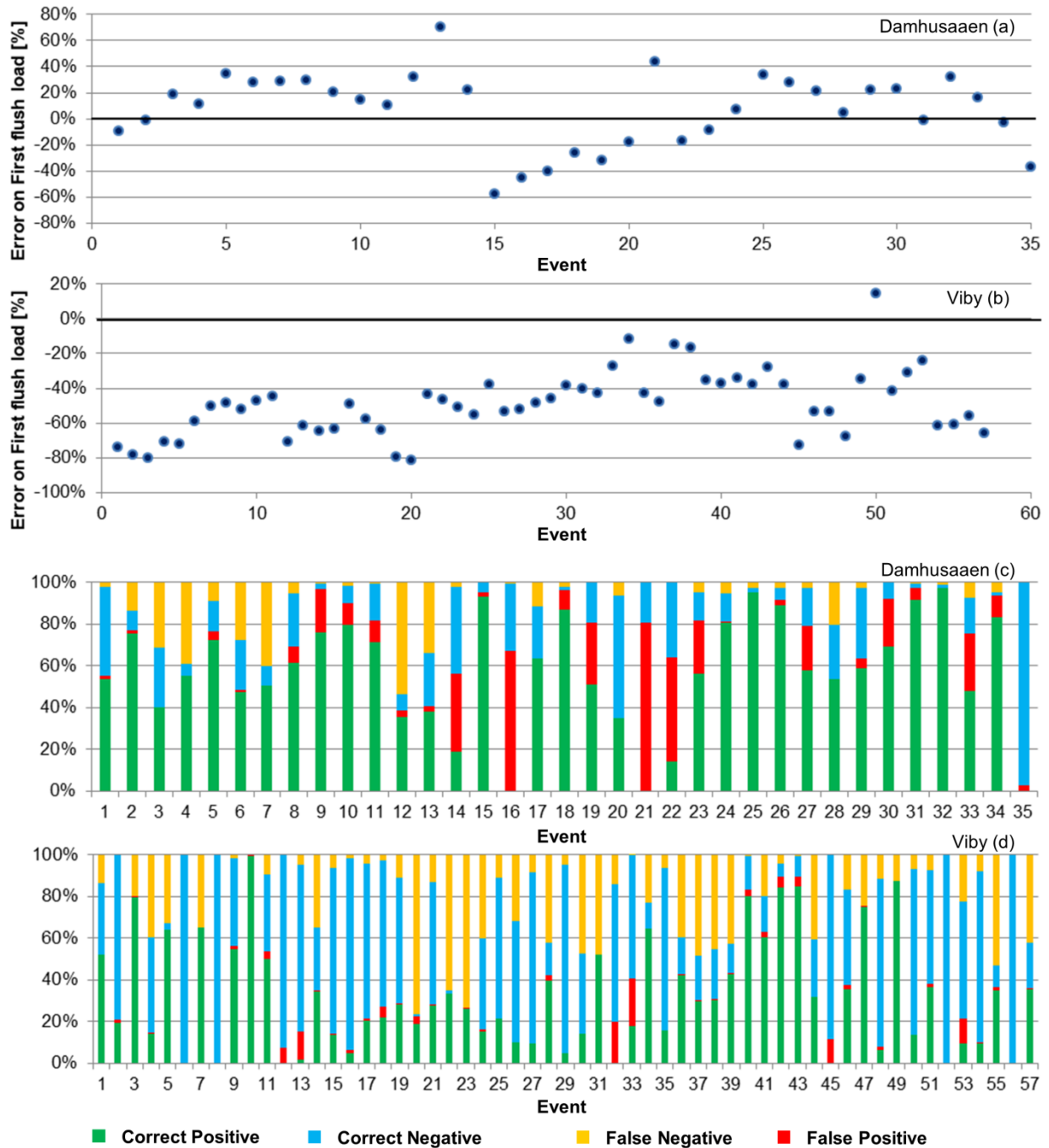
328  
329 **Figure 4.** Performance of the forecast model during the simulation period for Damhusaaen (a,b) and  
330 Viby (c,d). Each red dot represents the average performance for a given day, a blue background  
331 indicates wet periods, brown lines indicate sensor calibrations, and green lines indicate sensor  
332 cleaning (no calibration). Information on maintenance in Viby before November 2018 is missing.  
333

### 334 Performance during wet weather events

335 Figure 5 provides an overview of the forecast model performance regarding its potential  
336 applications for online control applications (e.g. controlling aeration in case of first flush

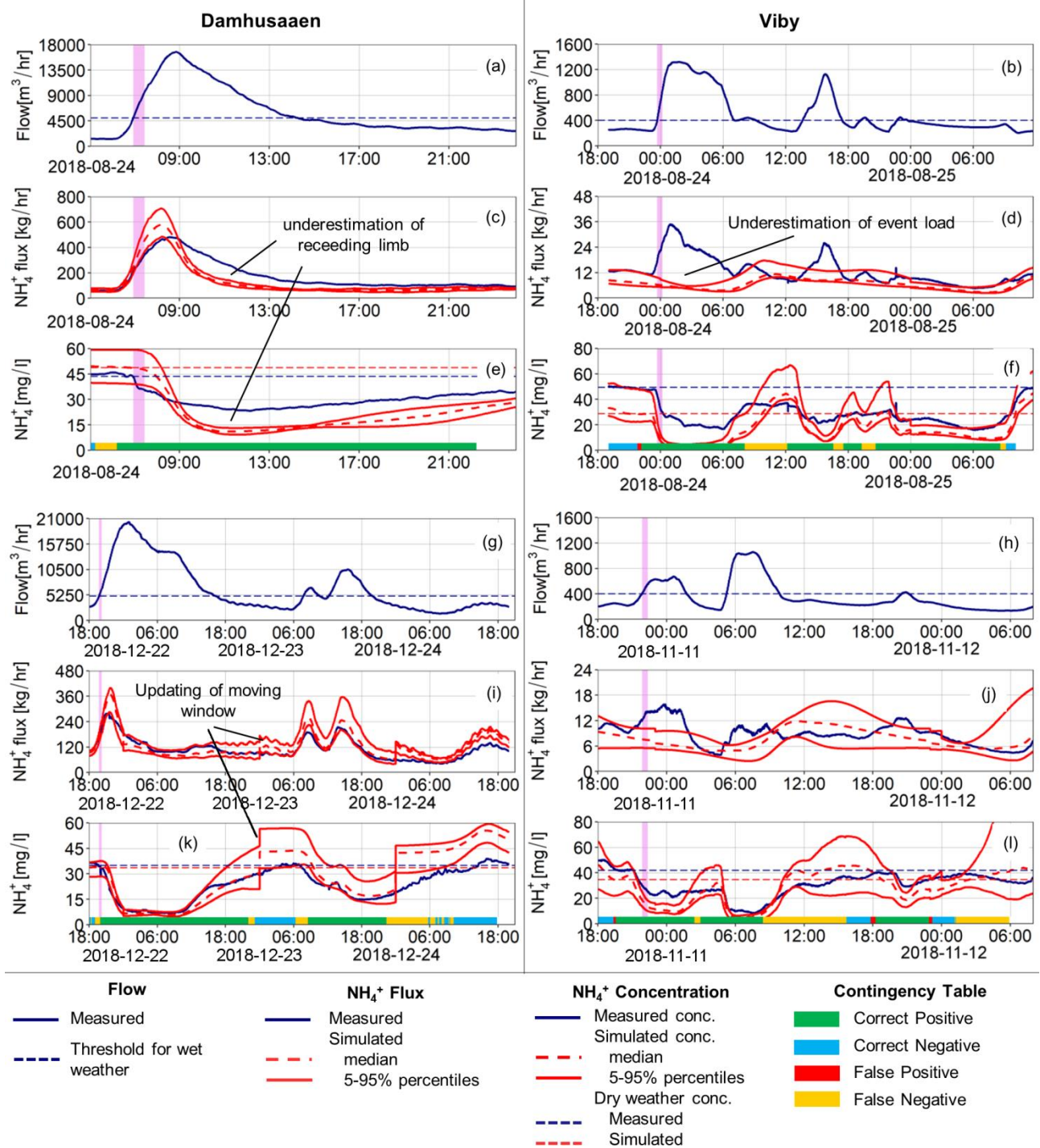
---

337 phenomena, or diverting low polluted flow to bypass structures). When looking at the prediction of  
338  $\text{NH}_4^+$  in the first phase of a rain event, the forecast model in Damhusaaen (Figure 5a) mostly  
339 remains in a  $\pm 40\%$  range. In the majority of the events, the load was overestimated. Conversely, in  
340 Viby (Figure 5b), the forecast model consistently underestimated the initial load. It should be  
341 pointed out that such performance analysis is strongly affected by the sensor calibration as some of  
342 the over/underestimation might be explained by events taking place shortly after sensor  
343 maintenance. Generally, the data show that rain-induced peaks have longer duration than 30  
344 minutes, i.e. the benefits of using such forecast for predictive control would be limited (after 30 min  
345 the wet-weather control would be fully operational). Figure 5c-d show the ability of predicting  
346 whether there are dilution effects from stormwater in each time step during an event. Here, the  
347 forecast model provided correct predictions (both correct positives and correct negatives) over 75%  
348 of the time for 22 events (63%) and 35 events (61%) in Damhusaaen and Viby, respectively. For  
349 some events the number of false positives (predicting a dilution while the concentration is still high,  
350 i.e. a prediction which might have negative consequences on the environment) was higher in  
351 Damhusaaen than in Viby. The number of events where the false positives exceeded 10% of the  
352 total event period was 13 (37%) in Damhusaaen and 5 (9%) in Viby. Figure 6 shows four examples  
353 of how the forecast model performed during different wet weather events. The examples suggest  
354 that the simple modelling approach based on dilution of ammonium loads is sufficient to grasp the  
355 dynamics at the beginning of a rain event, while it fails to represent the behaviour in the receding  
356 phase (Figure 6e).



357  
 358 **Figure 5.** Forecast model performance during wet weather events in Damhusaaen (a,c) and Viby  
 359 (b,d). (a,b) relative error in estimation of first flush load (first 30 min); graphical visualization of  
 360 contingency table for dilution prediction (c,d).  
 361

362 Such behaviour is in line with the findings of Langeveld et al. (2017), who added an additional term  
 363 to the model structure in order to obtain a better representation of the transition from the wet  
 364 weather concentrations back to dry weather values. Considering that the majority of online  
 365 applications for the proposed forecast model would focus on the initial phase of the event, structural  
 366 shortcomings at the end of the events are not expected to affect its performance. Furthermore, this  
 367 analysis illustrates the importance of evaluating the model performance in terms of its potential  
 368 applications, instead of limiting the analysis to an evaluation of the model residuals.



369  
 370  
 371  
 372  
 373  
 374  
 375  
 376  
 377  
 378  
 379  
 380

**Figure 6.** Examples of the forecast model predictions for four events at the inlet of Damhusaaen (left column) and Viby (right column). Measured flow (a-b,g-h); measured and simulated NH<sub>4</sub><sup>+</sup> fluxes (c-d,i-j); and concentrations (e-f,k-l), along with dry weather NH<sub>4</sub><sup>+</sup> concentrations used to define dilution events. The values from the corresponding contingency table are shown at the bottom of the concentration graph (e-f,k-l). Simulated values are described as median values (dashed line) and 90% prediction bounds (solid lines). Violet background identifies the first 30 min of the event used to evaluate first flush.

Figure 6(d,j) confirm the inadequacy of the model structure in Viby in representing the overall events. The available measurements suggest an increase in the ammonium loads, which might resemble the process described by Krebs et al. (1999). The model structure should therefore be

---

381 adapted accordingly. Nevertheless, Figure 6(f,l) show how the model was still capable of detecting  
382 the dilution during wet weather events. Figure 6(i,k) also highlight an issue linked to the moving  
383 window approach: the updating of the window can in fact result in discrete jumps of the predicted  
384 values. For an ensemble-based approach as the one in this study, these variations might be reduced  
385 by increasing the size  $n$  of the window.  
386

### 387 **Research gaps and future developments**

388 The available results show how the predictions of the proposed setup are strongly dependent on the  
389 signal provided by the ion-selective sensors and by the maintenance operations. As pointed out by  
390 Cecconi et al. (2019), excessive maintenance and/or improper sensor calibration might significantly  
391 decrease the reliability of ammonium measurements. Furthermore, the performance of the forecast  
392 model cannot be evaluated in a complete manner, since a major cause of poor indicator values is  
393 due to changes in the signal rather than in the model structure and/or parameters. Possible  
394 improvement of the proposed approach might include:

- 395 • Correction and transformation of the signal from the ion-selective sensor. Ideally, the raw signal  
396 from the sensor could provide a more reliable data source compared to the existing situation. A  
397 follow-up study on how to correct the raw ISE-based signal is currently being undertaken, as all  
398 the following improvements require a good quality dataset.
- 399 • Variable uncertainty description: the proposed ensemble approach equally weighs all the days in  
400 the calibration window. Approaches such as exponential filtering, weights on most recent days,  
401 etc. can be used to increase the importance of the most recent data for cases where this is  
402 desired.
- 403 • Use of stochastic models that combine a deterministic model with a stochastic term capable of  
404 describing the natural variability of the  $\text{NH}_4^+$  concentrations. Possible techniques include the so-  
405 called grey-box models or the external bias description (Del Giudice et al., 2015).
- 406 • A thorough evaluation of the influence of the different model parameterizations on the resulting  
407 predictions. The effect of the length of the moving window, the number of ensemble members,  
408 the intervals used in the parameter estimation, etc. should be fully evaluated. This would  
409 provide robust guidelines for a wide application of the proposed method to other systems.
- 410 • Performance evaluation of the proposed approach at CSO structures, i.e. where the installation  
411 of a permanent online  $\text{NH}_4^+$  sensor is less likely compared to WWTPs. Here the model would  
412 use historical data from monitoring campaigns of limited duration (e.g. an online sensor  
413 installed over a 2-3 months period) to forecast  $\text{NH}_4^+$  concentrations. The duration of the  
414 historical dataset should be sufficient to confidently estimate representative daily profiles (and  
415 their variations).
- 416 • Performance evaluation using real flow forecasts, based on e.g. radar rainfall forecasts or  
417 numerical weather predictions. There is ample research on flow uncertainty estimation, and this  
418 comparison could show if the uncertainties discussed here are significant compared with those  
419 related to the rainfall forecasts, which are known to be very large.
- 420 • Performance evaluation based on event definitions that are not strictly linked to the plant  
421 operational settings. For example, a variable flow threshold, defined on the actual dry weather  
422 flow conditions rather than the used fixed value, could improve the understanding of the model  
423 behaviour in wet weather.
- 424 • Modification of the model structure by including additional terms, such as those included in the  
425 model from Langeveld et al. (2017). This would expand the applicability of the model to other  
426 applications outside WWTP control (e.g. for quantification of CSO and bypass load)

427  
428

---

## 429 CONCLUSIONS

430 This work investigated the performance of simple model for online prediction of  $\text{NH}_4^+$   
431 concentrations intended for real time control applications. The analysis of the forecast model results  
432 showed that:

- 433 • The analysis of data from two Danish WWTPs showed high inter-diurnal variations in the  
434 incoming ammonium loads. This underlines the importance of using an uncertainty-based  
435 approach, which explicitly accounts for this natural variability.
- 436 • The simple structure of the model (based on Fourier series) should be adapted to the specific  
437 locations of the sensors and/or to the characteristics of the catchment.
- 438 • Calibration of the ammonium ISE sensors significantly affected the model performance. The  
439 proposed data-driven forecast model uses data from previous calibration periods, and its  
440 capability of matching the measured values drops just after the sensor is calibrated. This  
441 suggests a strong need for new approaches that can reduce the impact of the sensor calibration  
442 on the operation of online forecast models.
- 443 • The performance of the forecast model in relation to potential online control strategies seems  
444 satisfactory. Specifically, the model provided good simulations of both the ammonium loads at  
445 the beginning of a rain event and the dilution induced by wet-weather events.

446  
447 Overall, the proposed data-driven forecast model creates interesting opportunities for online  
448 forecasts of WWTP influent quality. Although further research is needed to improve the accuracy of  
449 the forecast model in terms of predicted concentrations, it can already open various possibilities for  
450 the implementation of online control strategies. The forecast model can also be applied for  
451 forecasting of incoming  $\text{NH}_4^+$  loads and concentrations, creating new opportunities for Model  
452 Predictive Control of WWTPs.

## 453 ACKNOWLEDGEMENT

454  
455 This research was financially supported by the Innovation Fund Denmark through the Water Smart  
456 Cities (WSC) project [grant number 5157-00009B]. The authors thank Tomas Trabjerg (Aarhus  
457 Vand A/S) for the detailed information regarding the measurements campaign at the Viby WWTP  
458 and Anders Breinholt (HOFOR. Hovedstadsområdet Forsyningsselskab) for the support in the  
459 Damhusaaen case study.

## 460 REFERENCES

- 461  
462  
463  
464 Ahm, M., Thorndahl, S., Rasmussen, M. R., Bassø, L. (2013) Estimating subcatchment runoff coefficients using  
465 weather radar and a downstream runoff sensor. *Water Science and Technology*, 68(6), 1293–1299.
- 466 Alferes, J., Tik, S., Copp, J., Vanrolleghem, P. A. (2013) Advanced monitoring of water systems using in situ  
467 measurement stations: data validation and fault detection. *Water Science and Technology*, 68(5), 1022–1030.
- 468 Bechmann, H., Nielsen, M. K., Madsen, H., Kjølstad Poulsen, N. (1999) Grey-box modelling of pollutant loads from a  
469 sewer system. *Urban Water*, 1(1), 71–78.
- 470 Bennett, N. D., Croke, B. F. W., Guariso, G., Guillaume, J. H. A., Hamilton, S. H., Jakeman, A. J., Marsili-Libelli, S.,  
471 Newham, L. T. H., Norton, J. P., Perrin, C., Pierce, S. A., Robson, B., Seppelt, R., Voinov, A. A., Fath, B. D.,  
472 Andreassian, V. (2013) Characterising performance of environmental models. *Environmental Modelling and  
473 Software*, 40, 1–20.
- 474 Cecconi, F., Reifsnnyder, S., Ito, Y., Jimenez, M., Sobhani, R., Rosso, D. (2019) ISE-ammonium sensors in WRRFs:  
475 field assessment of their influencing factors. *Environmental Science: Water Research & Technology*, 5(4), 737–746.
- 476 Flores-Alsina, X., Saagi, R., Lindblom, E., Thirsing, C., Thornberg, D., Gernaey, K. V., Jeppsson, U. (2014) Calibration  
477 and validation of a phenomenological influent pollutant disturbance scenario generator using full-scale data. *Water  
478 Research*, 51(0), 172–185.
- 479 Gernaey, K. V., Flores-Alsina, X., Rosen, C., Benedetti, L., Jeppsson, U. (2011) Dynamic influent pollutant disturbance  
480 scenario generation using a phenomenological modelling approach. *Environmental Modelling & Software*, 26(11),  
481 1255–1267.

---

482 Del Giudice, D., Löwe, R., Madsen, H., Mikkelsen, P. S., Rieckermann, J. (2015) Comparison of two stochastic  
483 techniques for reliable urban runoff prediction by modeling systematic errors. *Water Resources Research*, 51(7),  
484 5004–5022.

485 Haimi, H., Mulas, M., Corona, F., Vahala, R. (2013) Data-derived soft-sensors for biological wastewater treatment  
486 plants: An overview. *Environmental Modelling & Software*, 47, 88–107.

487 Hoppe, H., Messmann, S., Giga, A., Gruening, H. (2011) A real-time control strategy for separation of highly polluted  
488 storm water based on UV-Vis online measurements - from theory to operation. *Water Science and Technology*,  
489 63(10), 2287–2293.

490 Krebs, P., Holzer, P., Huisman, J. L., Rauch, W. (1999) First flush of dissolved compounds. *Water Science and*  
491 *Technology*, 39(9), 55–62.

492 Kusiak, A., Verma, A., Wei, X. (2013) A data-mining approach to predict influent quality. *Environmental Monitoring*  
493 *and Assessment*, 185(3), 2197–2210.

494 Langeveld, J., Van Daal, P., Schilperoort, R., Nopens, I., Flameling, T., Weijers, S. (2017) Empirical sewer water  
495 quality model for generating influent data for WWTP modelling. *Water*, 9(7), 491.

496 Langergraber, G., Alex, J., Weissenbacher, N., Woerner, D., Ahnert, M., Frehmann, T., Halft, N., Hobus, L., Plattes,  
497 M., Spering, V., and Winkler, S. (2008) Generation of diurnal variation for influent data for dynamic simulation.  
498 *Water Science and Technology*, 57(9), 1483–1486.

499 Martin, C., Vanrolleghem, P. A. (2014) Analysing, completing, and generating influent data for WWTP modelling: A  
500 critical review. *Environmental Modelling & Software*, 60, 188–201.

501 Métadier, M., Bertrand-Krajewski, J. L. (2012) The use of long-term on-line turbidity measurements for the calculation  
502 of urban stormwater pollutant concentrations, loads, pollutographs and intra-event fluxes. *Water Research*, 46(20),  
503 6836–6856.

504 Newhart, K. B., Holloway, R. W., Hering, A. S., Cath, T. Y. (2019) Data-driven performance analyses of wastewater  
505 treatment plants: A review. *Water Research*, 157, 498–513.

506 Nielsen, M. K., Onnerth, T. B. (1995) Improvement of a recirculating plant by introducing star control. *Water Science*  
507 *and Technology*, 31(2), 171–180.

508 Schilperoort, R. P. S., Dirksen, J., Langeveld, J. G., Clemens, F. H. L. R. (2012) Assessing characteristic time and space  
509 scales of in-sewer processes by analysis of one year of continuous in-sewer monitoring data. *Water Science and*  
510 *Technology*, 66(8), 1614–1620.

511 Stentoft, P. A., Munk-Nielsen, T., Steen Mikkelsen, P., Madsen, H. (2017) “A Stochastic Method to Manage Delay and  
512 Missing Values for In-Situ Sensors in an Alternating Activated Sludge Process” in *Proceedings of 12<sup>th</sup> IWA*  
513 *Specialized Conference on Instrumentation, Control and Automation, Quebec City, Canada, 11<sup>th</sup>-14<sup>th</sup> June 2017*.

514 Stentoft, P. A., Munk-Nielsen, T., Vezzaro, L., Madsen, H., Mikkelsen, P. S., Møller, J. K. (2019) Towards model  
515 predictive control: online predictions of ammonium and nitrate removal by using a stochastic ASM. *Water Science*  
516 *and Technology*, 79(1), 51–62.

517 Talebizadeh, M., Belia, E., Vanrolleghem, P. A. (2016) Influent generator for probabilistic modeling of nutrient  
518 removal wastewater treatment plants. *Environmental Modelling & Software*, 77, 32–49.

519 Vezzaro, L., Lund Christensen, M., Thirsing, C., Grum, M., Mikkelsen, P. S. (2013) Water quality-based real time  
520 control of integrated urban drainage: a preliminary study from Copenhagen, Denmark. *Procedia Engineering*, 70,  
521 1707–1716.

522 Yu, T., Yang, S., Bai, Y., Gao, X., and Li, C. (2018) Inlet water quality forecasting of wastewater treatment based on  
523 kernel principal component analysis and an extreme learning machine. *Water (Switzerland)*, 10(7), 873.

524 Yuan, Z., Olsson, G., Cardell-Oliver, R., van Schagen, K., Marchi, A., Deletic, A., Ulrich, C., Rauch, W., Liu, Y., and  
525 Jiang, G. (2019) Sweating the assets – The role of instrumentation, control and automation in urban water systems.  
526 *Water Research*, 155, 381–402.

527

## SUPPLEMENTARY INFORMATION

**Title:** Evaluating the performance of a simple phenomenological model for online forecasting of ammonium concentrations at WWTP inlets

**Authors:** Luca Vezzaro, Jonas Wied Pedersen, Laura Holm Larsen, Carsten Thirsing, Lene Bassø Duus, and Peter Steen Mikkelsen

**Table S1.** Main technical data of the ISE sensors used in the two catchments (from the producers' data sheets)

		Unit	Damhusaaen	Viby
Sensor range (resolution)	NH <sub>4</sub> <sup>+</sup>	mg/l	0-1000	0.1-100 (0.1)
	K <sup>+</sup>	mg/l	0-1000	1-1000 (1)
	Temperature	°C	-	0-40 (0.1)
Sensor operating range	pH	-	5-9	4-8.5
	Temperature	°C	2-40	0-40
Sensor precision		mg/l	±5%	±5% (in domestic wastewater)
Response time		minutes	< 3	-

**Table S2.** Summary of rainfall data collected by the station of the Water Pollution Committee of the Society of Danish Engineers (Jørgensen et al., 1998) during the simulated period (20180601-20190515)

Rain gauge	Yearly rainfall [mm] <sup>a</sup>	No of rainfall events				
		Total	>1 mm	>2 mm	>3 mm	>4 mm
Damhusaaen						
5699 Gladsaxe Stavnbjerg Alle	660	190	93	64	40	29
5705 Åvenningen	644	192	95	63	43	30
5710 Rødovre Vandværk	645	194	91	63	41	31
5771 Træholmen	646	188	83	54	44	33
5775 Hvidovre Vandværk	643	194	97	63	43	32
Viby						
5177 Viby J Renseanlæg	665	187	92	58	37	24

<sup>a</sup> Obtained from Spildevandskomitéen (2014)

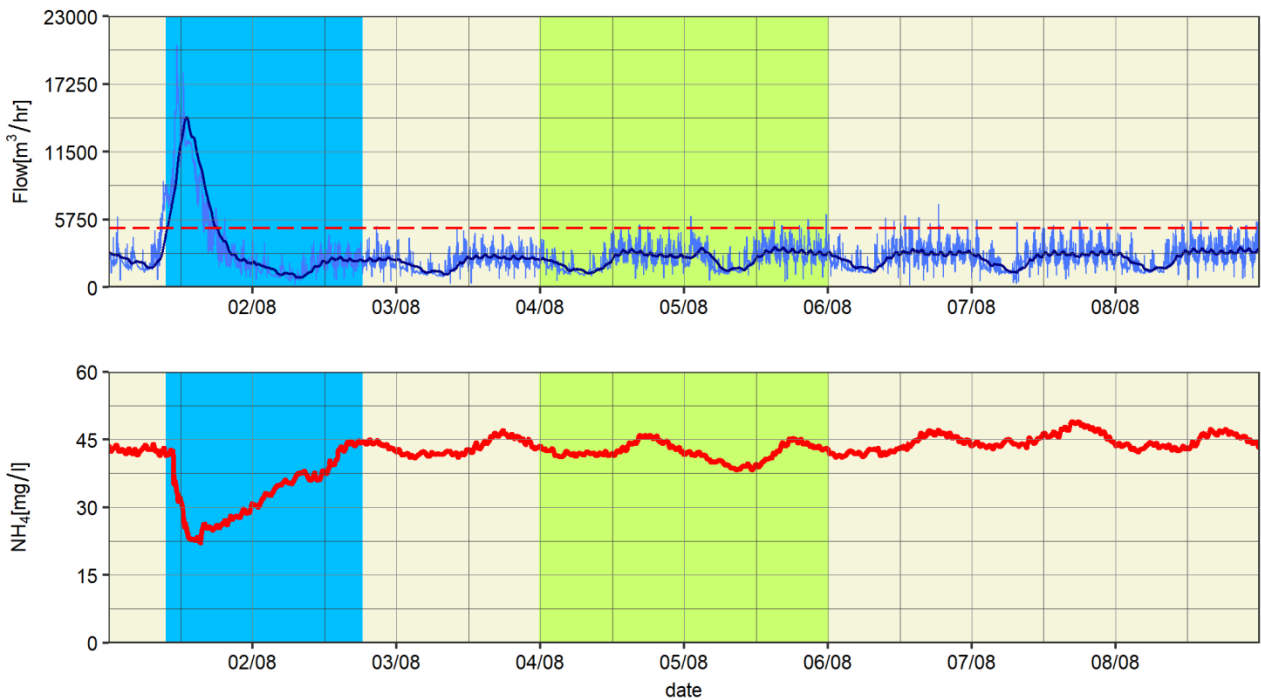


**Figure S1.** Measured flow (above) and ammonium (below) at Damhusaen in the period from 2018/08/01 to 2018/08/09. Light blue line: raw flow data; dark blue line: filtered flow data. Red dashed line: threshold for the definition of a wet-weather event. Wet weather events are shown with light blue background, weekends are shown with green background. Note the several exceedances of the wet-weather data threshold by the raw data in the period from 2018/08/05 to 2018/08/08.

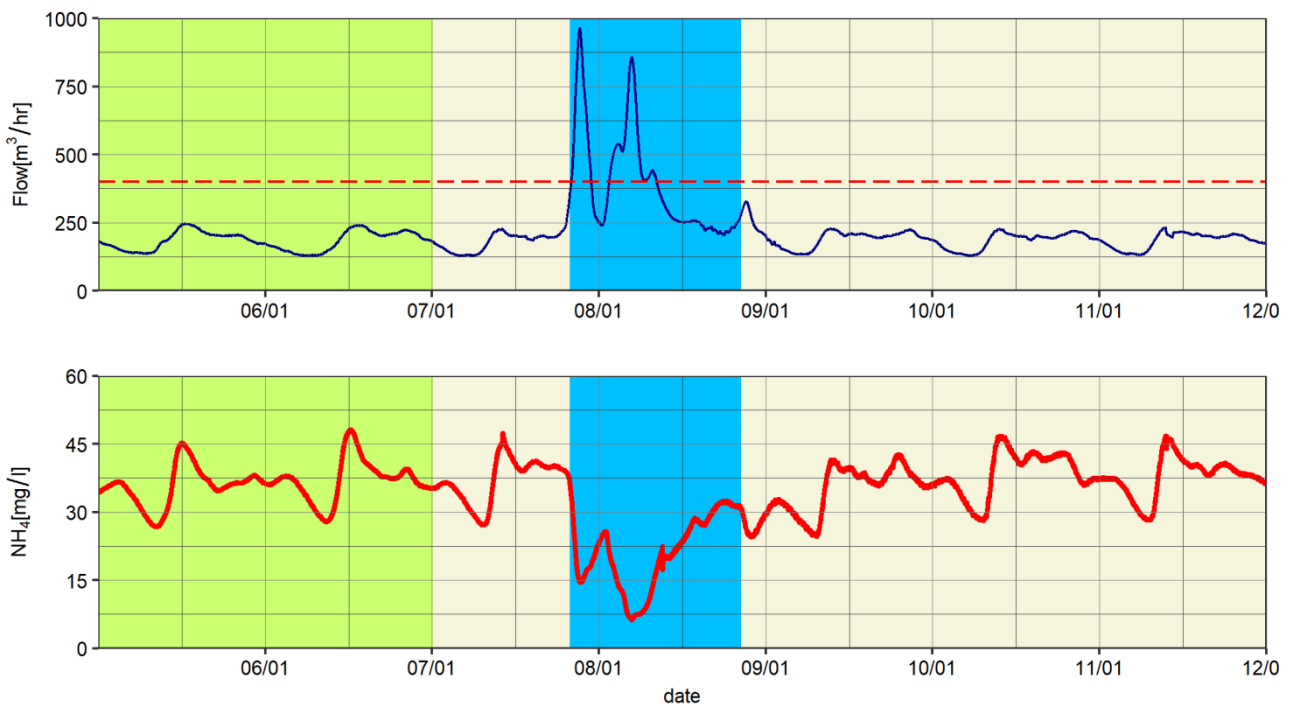


**Figure S2.** Measured flow (above) and ammonium (below) at Viby in the period from 2019/01/05 to 2019/01/12. Blue line: flow data. Red dashed line: threshold for the definition of a wet-weather event. Wet weather events are shown with light blue background, weekends are shown with green background.

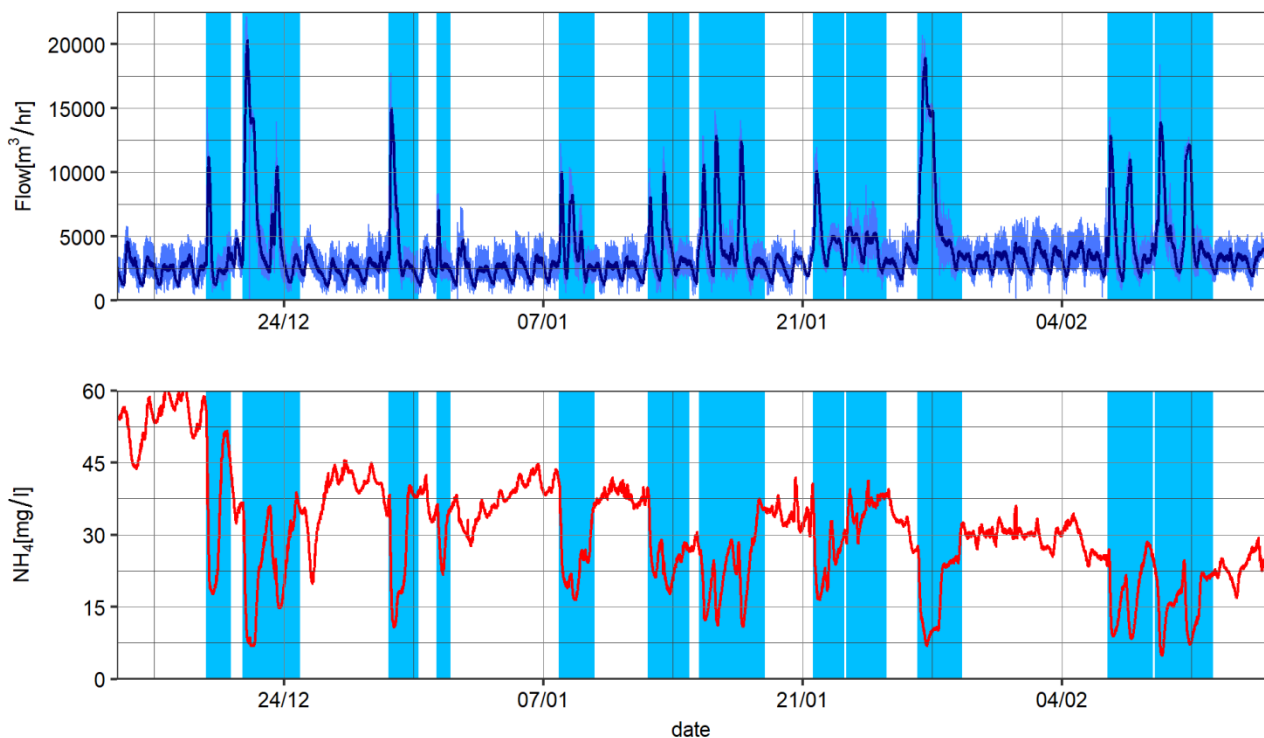


**Figure S3.** Measured flow (above) and ammonium (below) at Damhusaaen in the period from 2018/12/15 to 2019/02/15. Light blue line: raw flow data; dark blue line: filtered flow data. Wet weather events are shown with light blue background.

## References

- Jørgensen, H. K., Rosenørn, S., Madsen, H., Mikkelsen, P. S. (1998) Quality control of rain data used for urban runoff systems. *Water Science and Technology*, **37**(11), 113–120.
- Spildevandskomitéen (2014) Skrift 30 - Opdaterede klimafaktorer og dimensionsgivende regnintensiteter (in Danish). Water Pollution Committee of the Society of Danish Engineers, Guideline 30: updated climate factors and dimensioning rainfall intensities (available at <https://ida.dk/om-ida/spildevandskomiteen/skrifter-spildevandskomiteen#se-og-hent-skrifter>, last accessed 2020-01-26).